PAPER 94 – SYNTHESIS AND CHARACTERIZATION OF CNTS/TIO$_2$ NANOCOMPOSITE FOR FORMULATION OF HYBRID NANOFLUID FOR MACHINING CFRPS

S. A. Lawal[1,6], R. O. Medupin[2*], U. G. Okoro[1], O. Adedipe[1], J. Abutu[3], J. O. Tijani[4], A. S. Abdulkareem[5], M. B. Ndaliman[1]

[1]Department of Mechanical Engineering, Federal University of Technology, Minna, Nigeria.
[2]Department of Materials and Metallurgical Engineering, Federal University of Technology, Owerri, Nigeria.
[3]Department of Mechanical Engineering, Taraba State University, Jalingo, Nigeria.
[4]Department of Chemistry, Federal University of Technology Minna, Nigeria.
[5]Department of Chemical Engineering, Federal University of Technology, Minna, Nigeria.
[6]Department of Mechanical Engineering, University of Mines and Technology, Tarkwa, Ghana
[*]Email: rasaq.medupin@futo.edu.ng

ABSTRACT
Removal of heat from cutting zones raises concerns in machining carbon fibre reinforced plastics (CFRPs). Therefore, this has necessitated increased search for sustainable and cost-effective cooling agents. In this study, carbon nanotubes (CNTs) and TiO_2 were synthesised using sol-gel and Central Composite Design and characterised to form different compositions of TiO_2/CNTs (9:1, 7:3, and 5:5) nanocomposites. The nanocomposites were characterized using Brunauer-Emmett-Teller (BET), HESEM/EDX, XRD and FTIR to investigate their stability as suitable fillers in base-oils. The FTIR spectra for TiO_2/CNTs revealed that the composites have absorption peaks corresponding to C=C and Ti-O bonds; giving rise to peaks assigned to Ti-O-C and C-O bonds. The diffraction peaks of anatase are clearly identified and the diffraction peaks assigned to CNTs are barely seen as a result of overlapping of the main peaks of CNTs with the peaks of TiO_2. The study established that the challenges common to individual NCs are sufficiently addressed with hybrid NCs TiO_2/CNTs (5:5) NC offering an overriding advantage over other nanocomposites as heat removing agent owing to its largest surface area, pore volume and as the most stable nanosuspension. It can, therefore, be concluded that TiO_2/CNTs nanocomposites have high prospect for reinforcing base oils for effective machining.

KEYWORDS: Synthesis, Characterisation, Carbon nanotubes, Titanium oxide, Nanocomposites, Machining

1. INTRODUCTION

Carbon fibre reinforced plastics (CFRPs) have been established as indispensable materials for many applications in engineering. Their outstanding performance in national defence, aerospace and upscale civilian products earns them their current status in manufacturing technology (Zheng et al., 2022). However, until recently, machining of CFRPs has received less attention than they actually deserve as a material with comparative advantages (Erturk et al., 2021). Researchers who have investigated machining of CFRPs with conventional cutting fluids decried the associated challenges and call for more studies to unravel the uncharted waters (Elgnemi et al., 2021; Wang et al., 2018; Zhang et al., 2017). Most of the orthodox cutting fluids are proven to have repeatedly fail to sustain their relevance in the current efforts towards achieving the UN's Sustainable Development Goals on responsible consumption and production (SDG #12).

Quick and easy removal of heat from cutting zones during machining affect the level of success of the process in terms of tool life, speed of cutting as well as surface finish. Sankaranarayanan et al. (2021) reported on the preference of bio-oil-based cutting fluids to proffer solutions to numerous health hazards associated with synthetic cutting fluids in pursuance of sustainable green manufacturing. Even though synthetic and vegetable oil perform excellent momentary cooling functions during machining, chemical imbalance which often triggers corrosion process renders them ineffectual in the present environmentally conscious world (Pimenov et al., 2021). Therefore, nanofluids are currently being advanced to address issues around quick heat removal from tool/workpiece interface by leveraging large surface areas provided by nanoparticles (NPs). This is expected to facilitate quick removal of heat and also help to reduce the quantity of fluids needed for a particular machining process (Patole et al., 2021). The volume of cutting fluids needed as well as the volume released to the immediate environment after being used are also significantly reduced; hence environmental pollution is effectively addressed in the same manner cost is also sufficiently managed (Ni et al., 2021; Haq et al., 2021). It is in line with this principle that the Minimum Quantity Lubrication (MQL) technique was established to further optimize machining parameters (Usha & Srinivasa Rao, 2019). MQL is an environment-friendly and cost-effective alternative to flooding and dry cutting fluid application (Agrawal & Patil, 2018). It is a machining process that is consistent with cleaner and responsible production in the context of sustainable production.

However, more recently, a more excellent way of performing the dual functions of heat removal and lubrication during machining has been launched and is currently receiving more attention from the research world (Gao et al., 2021). While the fluid lubricates the cutting interface, the nanofillers convey heat away from the cutting zone; making machining experience rather seamless and fast; thereby extending tool life and enhancing surface finish (Singh et al., 2021). This is termed nanofluid-MQL (nMQL). Kumar et al. (2023), in a recent study, described nMQL as the novel chapter of sustainable machining. The process involves spraying nanofluids mist on to the tool work interface during machining as the sliding friction between the tool work is converted to rolling friction and reduces friction coefficient significantly; hence giving rise to low cutting forces (Bai et al., 2019; Osman et al., 2020; Jamil MKhan et al., 2020; Lawal et al., 2023). Venkatesan et al. (2020) conducted a comparative study on certain machining parameters under dry and MQL. Their observation on turning operation under nMQL shows that MQL prevents wear mechanism which is a peculiar drawback with dry machining. This indicates that the use of nMQL is a step in the right direction in sustainable machining of difficult-to-machine materials for industrial applications. While also investigating the approach, Gao et al. (2021) observed that the optimization of the nanofluids under high pressure air flow addresses the problem of unsatisfactory heat transfer capacity of MQL in the machining zone and improves the lubrication performance of the interface between the tool and the workpiece. While acknowledging the possibility of taking advantage of different physical and chemical properties of NPs to form hybrid nanofluids, Gao et al. (2020) submitted that the use nMQL technique could lower processing damage such as resin coating, multi-fibre block pull-out, as well as pits. Therefore, it can be concluded that nMQL is the undisputable future of CFRPs machining.

Excellent as nMQL technique may seem, a number of challenges have been identified with the process of producing hybrid nanofluids. Production of standard nanosuspension remains an age-long procedural challenge. Abubakre et al. (2023) agreed with an earlier work by Urmi et al. (2021) on the difficulties associated with the attainment of long-term stability of hybrid nanofluids, which is one of the requirements of hybrid nanofluids applications. This quality of the nanofluids is important in that it improves its thermal behaviour during applications. Therefore, addressing the stability issue is vital to carrying out quality machining. From the literature, external force, stirring and ultrasonication can be deployed to break the bonds that hold NPs together provided the duration for each activity is addressed (Medupin et al., 2019; Ma et al., 2022). Hence the question of time remains a huge gap in the literature. Hence, given the vital role NPs play in the achievement of excellent clean machining via nMQL technique, the processes leading to the production of NPs deserves all the needed attention. It is in keeping with this, therefore, that this study is designed to synthesise and characterise high quality carbon nanotubes (CNTs), TiO_2 and their nanocomposites (NCs) for the development of hybrid nanofluids for CFRPs machining.

2. MATERIALS AND METHODS

All reagents used in this study were of analytical grade with percentage purity in the range of 95%-99.98%. They were sourced from Sigma Aldrich Chemicals Nigeria, a world class distributor of chemicals and other product and used without any further purification. The chemicals used in this experiment include titanium (IV) isopropoxide ($Ti\{OCH(CH_3)_2\}_4$, methanol (CH_3OH), sodium hydroxide pellets (NaOH), hydrochloric acid (HCl) and sodium dodecyl sulfate (SDS) as well as deionized and distilled water.

2.1 Synthesis of TiO_2 nanoparticles

Central Composite Design (CCD) based on Response Surface Method (RSM) was used for biosynthesis of TiO_2 NPs using sol-gel method as shown in Tables 1 and 2. A known volume of titanium isopropoxide was measured into a 250 cm^3 beaker containing a specific volume of extract from plant and stirred on a magnetic stirrer. The mixture was adjusted to the desired pH using NaOH and HCl solution under continuous stirring. The resulting mixture was washed with de-ionized water, dried at 105 ^oC in an oven for 12 h, and calcined at 450 ^oC for 3 h.

Table 1: 2^4 factorial design matrices

Coded value	Volume of extract (cm^3)	Volume of precursor (cm^3)	Stirring time (min)	pH
– Level	50	5	100	2
+ Level	80	8	200	12

Table 2: Experimental run for the biosynthesis of TiO_2 nanoparticles

Selected Run	Volume of extract (cm^3)	Stirring time (min)	Volume of precursor (cm^3)	pH	Crystallite size (nm)
3	65	100	6.5	12	18.92
6	50	100	6.5	7	10.20
9	80	150	6.5	12	16.41

13	65	200	6.5	2	8.09
15	65	200	8.0	7	11.05
17	65	100	8.0	7	9.70
19	65	150	5.0	2	7.64
21	50	150	6.5	12	14.09
25	65	200	5.0	7	10.15

2.2 Synthesis and purification of Carbon Nanotubes

A weight of 14.53 g of Ni and 20.2 g of Fe were dissolved in 100 ml of distilled water, and 10 g of kaolin was added to the mixture and shaken with orbital shaker at 200 rpm for 1 h. The mixture was allowed to cool before decanting and kept in the oven for 12 h at 120 °C to dry. The dried mixture was grounded and screened through a 150 μm sieve. The resulting fine powder (catalyst) was then calcined for 16 h at 500 °C to remove the nitrate content. Afterwards, the dried catalyst was then grounded to forestall the incidence of agglomeration that may hamper the interaction between carbon source and the surface mixture. Carbon nanotubes (CNTs) was then synthesized by decomposition acetylene (a carbon source) in a tubular quartz reactor placed horizontally in a furnace. The furnace was electronically controlled such that the heating rate, reaction temperature and gas flow rates were adequately regulated.

1.0 g of catalyst was spread in a quartz boat (11 cm × 2.6 cm) to form a thin layer and then placed in the centre of the quartz tube. The furnace was heated up at 10 °C/min while argon (Ar) was concurrently passed through the system at 30 ml/min. This was to ensure both inert contaminant-free furnace atmosphere and prevent oxidation of the samples before and after the reaction. Once the temperature reached the set reaction temperature of 750 °C, the argon flow rate was adjusted to 230 ml/min. C_2H_2 was then introduced at a flow rate of 150 ml/min and 200 ml/min in order to initiate CNTs growth. After 90 min reaction time, C_2H_2 flow was halted as the furnace cooled down to room temperature under a continuous flow of argon at 30 ml/min flow rate. The boat was withdrawn from the reactor to harvest the carbon deposit along with the catalyst. CNTs yield (%) was calculated based on the relationship expressed in Equation 1.

A 2.0 g measure of CNTs was loaded into a beaker containing 200 ml of 3M NaOH solution in order to remove the transition metal (Fe-Ni) catalysts and the support material (kaolin). The solution was then stirred using magnetic stirrer for 3 hours and allowed to settle. Subsequently, the solution was filtered and washed with distilled water to ensure a neutral pH. It was then dried at a temperature of 120 °C for 24 h. The CNTs was finally sonicated and kept in the shelf for further use.

2.3 Synthesis of nanocomposites

A known mass of synthesized CNTs and TiO_2 (TiO_2/CNTs) at different ratios were weighed in a ceramic mortar and crushed adequately with a pestle. The resulting mixtures for TiO_2/CNTs at 9:1, 7:3, and 5:5 ratios were compounded before analysis. In synthesising TiO_2/CNTs NCs, TiO_2/CNTs at 9:1, 7:3, and 5:5 ratios were compounded. At the same time, TiO_2 was dissolved in a suitable solvent and then added in droplets into the dispersed CNTs as sonication progresses and followed immediately with magnetic stirring. The suspension was transferred into round-bottom flask and refluxed at 200 °C in oil bath with magnetic stirring. Afterwards, the system was allowed to cool naturally to room temperature, filtered and washed with distilled water and ethanol several times. Subsequently, the resulted composite was dried at 100 °C and calcined at 550 °C.

2.4 Characterization of nanomaterials

Samples were characterized using Bruker AXS D8 Advance X-ray Diffractometer (XRD) with Cu Kα radiation to determine the phase and crystallite sizes of the NPs. Morphologies and structure of samples were characterized using Zeiss Auriga HRSEM with EDX. The EDX (operated at EHT for 20 kV), and the elemental composition of the samples was determined. The Brunauer-Emmett-Teller, BET surface area and pore size distributions of the samples were obtained from the plot of volume adsorbed versus relative pressure following the placement of 0.1 g sample in a tube after being degassed at 95 °C for 4 h to remove residual water and volatile compounds.

3 RESULTS AND DISCUSSION

2.2 XRD analysis of optimized CNTs, TiO_2 and TiO_2/CNTs

The factorial design of 2^4 factorials and experimental runs are presented in Tables 1 and 2 and used to investigate the influence of synthesis factors such as stirring time, pH, precursor volume, and extract volume on NPs yield. The crystallite size of TiO_2 is provided by XRD analysis. The phase composition estimated on the peak intensities was anatase, as presented in Fig. 1. Mean crystallite size was computed from full width at half maximum of related

diffraction anatase peak using Scherrer Debye equation (Equation 2). The smallest crystallite size was confirmed at an acidic medium (Table 2: run 19).

where is the crystallite size, is the shape factor (0.94), λ is the wavelength of the X-ray source, and is the full width at half maximum (FWHM).

Fig. 2 presents the XRD results of the CNTs, TiO_2, and TiO_2/CNTs NCs at different compounding ratios. XRD patterns reveal that mainly anatase peaks are found for the TiO_2 at 2 = 25.2°, 37.7°, 48°, and 54°. CNTs clearly displays two peaks at around 31.6° and 52.1°, which are indexed to the reflection of graphite of (002) and (100), respectively. For TiO_2/CNTs NCs, the diffraction peaks of anatase are clearly identified (Mustapha et al., 2020), and the diffraction peaks assigned to CNTs are barely seen (see Fig. 2(A)). This may be as a result of the overlapping of the main peaks of CNTs with the peaks of TiO_2 and is also attributable to the high intensity of the diffraction peaks of TiO_2 and low content of CNTs in the composites. Notably, the width of the XRD peaks at 35.03° and 57.5° was slightly broadened as CNTs were added to the NCs. This process implies that the introduction of CNTs markedly changes the NCs' crystalline size of TiO_2.

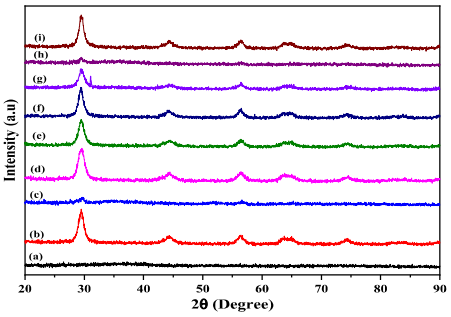

Fig. 1: XRD patterns of TiO_2 NPs for runs in Table 2

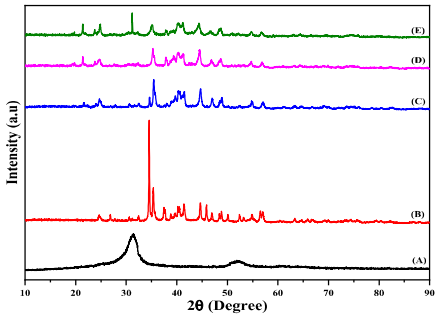

Fig. 2: XRD patterns of CNTs (A), TiO_2 (B), TiO_2/CNTs (9:1; 7:3; 5:5)

3.2 HRSEM/EDX of TiO_2, CNTs and TiO_2/CNTs

Fig. 3 presents HRSEM images of TiO_2, CNTs, and TiO_2/CNTs NCs at different ratios. The image shown in Fig. 3(a), the TiO_2 NPs, form a fleck-like structure and on the other hand, Fig. 3(b) reveals HRSEM image of tube-like CNTs with a diameter between 20 and 30 nm with a few agglomerated branches and tiny particles on the surface. The magnified images in Fig. 3(c-e) demonstrate that TiO_2 NPs are well dispersed on the surface of CNTs. The less identification of CNTs in the NCs was consistent with the TiO_2/CNTs content ratios in the samples, resulting in a well-homogeneous distribution of TiO_2 on the CNTs in TiO_2/CNTs (9:1) as shown in Fig. 3(c). Comparing the NCs with the TiO_2 NPs, the HRSEM image of TiO_2 presence voids or spaces between the particles; suggesting inter-particle porosity. The NCs suggest that the morphologies obtained for the NCs may be due to the interaction between TiO_2 and defect sites of the CNTs surface via binding by the intermolecular interaction.

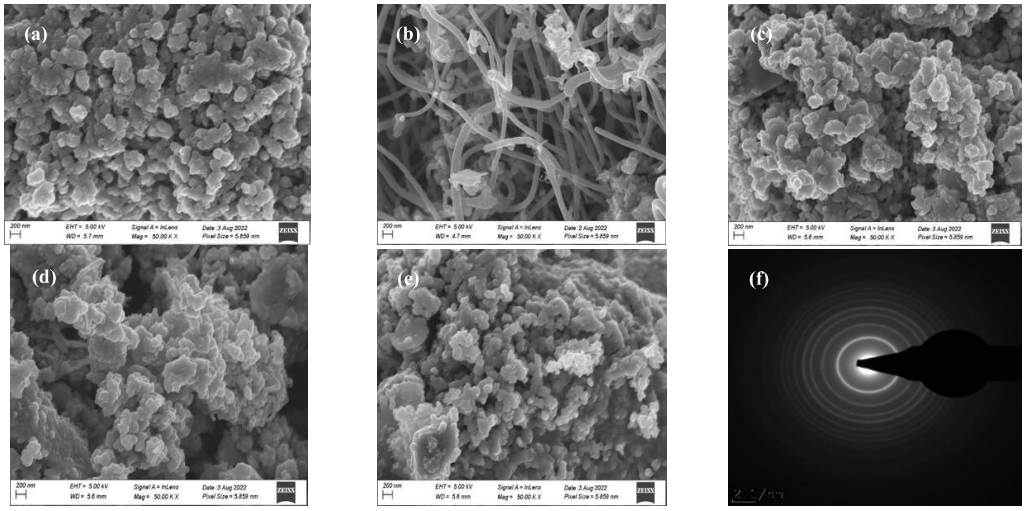

Fig. 3: HRSEM images of TiO_2 (a), CNTs (b), TiO_2/CNTs (9:1) (c), TiO_2/CNTs (7:3) (d), TiO_2/CNTs (5:5) (e)

The corresponding SAED pattern (Fig 3(f)) reflects MWCNTs, while the diffraction for anatase suggests the polycentric ring of TiO_2 as seen in the EDX spectra (Fig. 4). These were also confirmed by XRD analysis. The NCs also show polycentric rings of different reflection planes, which assume the nature of the TiO_2 dispersed in CNTs to form Ti-O-C and Ti-O-Ti networks. The EDX spectra (Fig. 4) indicate the Ti, C, and O are the predominant elements of the NCs in addition to trace elements from Ni salt and kaolin catalysts. The EDX analysis revealed that the presence of Ti content in the NCs composed followed the mass ratio of the composites.

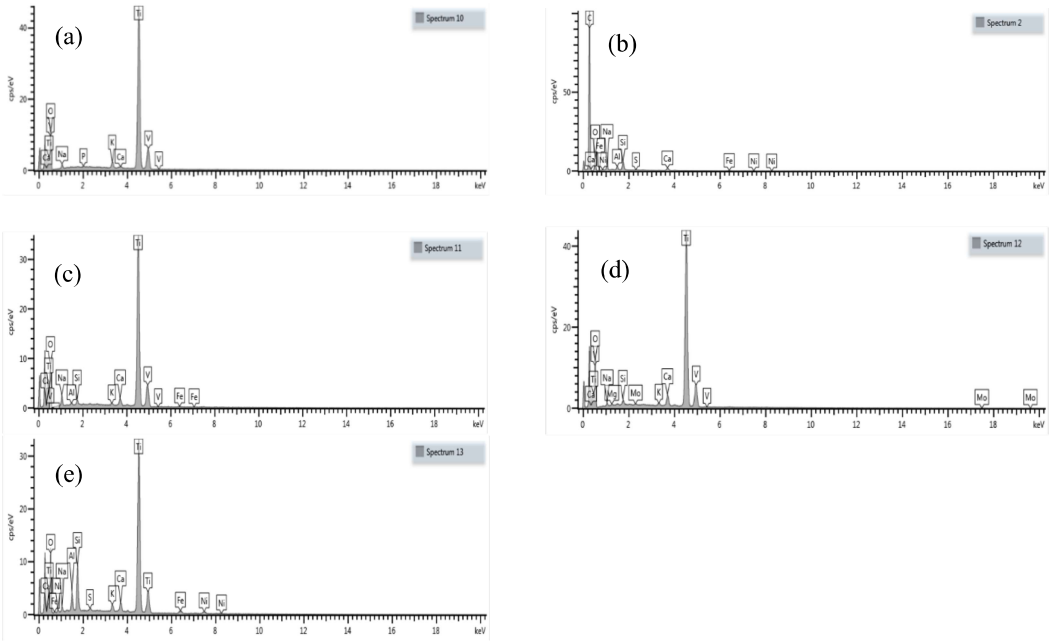

Fig. 4: EDX results of TiO_2 (a), CNTs (b), TiO_2/CNTs (9:1) (c), TiO_2/CNTs (7:3) (d), TiO2/CNTs (5:5) (e)

3.3 BET of TiO_2, CNTs and TiO_2/CNTs

Fig. 5 shows the N_2 adsorption-desorption isotherms of CNTs, TiO_2, and TiO_2/CNTs NCs while the BET-specific surface area, pore size, and pore volume are presented in Table 3. Based on the N_2 adsorption-desorption isotherm of TiO_2, the isotherms could be identified as the intermediate cases between hysteresis loop of type I where the two branches are almost vertical and parallel of a range of gas uptake and hysteresis loop of type IV where the branches stay nearly horizontal and parallel over a wide p/p^o range (D'Aloia et al., 2021). The isotherm identified for the CNTs is the type III isotherm as presented in Fig. 5(a). The isotherms resulting from the NCs are categorized as type II isotherms which can be ascribed to the combination of type I and type IV loops (Brockmann et al., 2020). This is explained by the fact that the isotherm of Fig. 5(e) is closer to type II than both TiO_2/CNTs (9:1) and TiO_2/CNTs. In Table 3, BET surface areas of the nanomaterials are presented. The surface area of TiO_2 is much higher than CNTs, indicating better textural properties and a wider range of applications. Also, the surface areas of the NCs increase as TiO_2 decreases relative to CNTs contents in the samples. This phenomenon could be caused by the separation of TiO_2 crystalline particles due to the addition of CNTs. Furthermore, the pore sizes reflect mesoporous nanomaterials which could favour mass transfer (Paumo et al., 2021). Pore volume of the NCs followed the same trajectory as the surface area and increase as CNTs content increases. This is attributable to the TiO_2 constantly occupying the reaction sites on the CNTs wall in accordance with an earlier work by Medupin et al. (2020).

Table 3: The summary of the BET results of CNTs, TiO_2, and TiO_2/CNTs

Sample	Surface area (m^2/g)	Pore size (nm)	Pore volume (cc/g)
CNTs	0.65	16.79	0.00276
TiO_2	127.62	6.648	0.296
CNTs/TiO_2 (1:9)	57.84	7.637	0.155
CNTs/TiO_2 (3:7)	71.19	8.412	0.195
CNTs/TiO_2 (5:5)	103.42	7.451	0.259

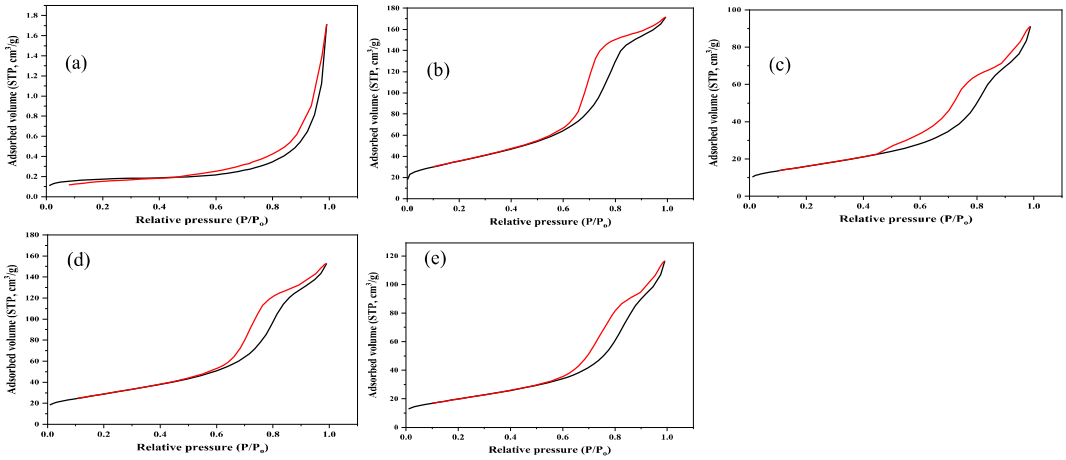

Fig. 5: N_2 Adsorption-desorption curves of CNTs (a), TiO_2 (b), TiO_2/CNTs (9:1) (c), TiO_2/CNTs (7:3) (d), TiO_2/CNTs (5:5) (e)

3.4 FTIR of TiO_2, CNTs and TiO_2/CNTs NCs

The FTIR spectra of TiO_2, CNTs, and TiO_2/CNTs are recorded and are shown in Fig. 6 to study the type of interactions that exist among the different constituents of the NCs and to determine their structure and functional groups. The absorption around 1630 cm^{-1} is assigned to the bending vibration of adsorbed water molecules (Fig. 6(a)). The broad band at the region of 950 cm^{-1} in the TiO_2 sample belongs to the characteristic vibration of the Ti–O–Ti network. It can be observed that the CNTs (Fig. 6(b)) show the C–C stretching bonds at 1650 cm^{-1} assigned as nanotube modes, and the peak in 1705 cm^{-1} is associated with C=O stretching of the carboxyl group as a characteristic of carboxyl functional groups (-COOH) (Medupin et al., 2017; Gopiraman et al., 2012; Shaban et al., 2020). The peaks around 3500-3300 cm^{-1} correspond to –OH stretching bond in hydroxyl and carboxyl groups indicative of the high presence of the groups. The FTIR spectra for the TiO_2/CNTs are shown in Fig. 6(c, d and e) reveals that the composites have absorption peaks corresponding to C=C and Ti-O bonds, giving rise to peaks assigned to Ti-O-C and C-O bonds (Pownraj & Valan Arasu, 2020; Khadom et al., 2022). These results demonstrate that the growth resulted in the formation of hetero-junction at the surface of the TiO_2 and CNTs, forming interfacial bonds in the matrices (Paumo et al., 2021).

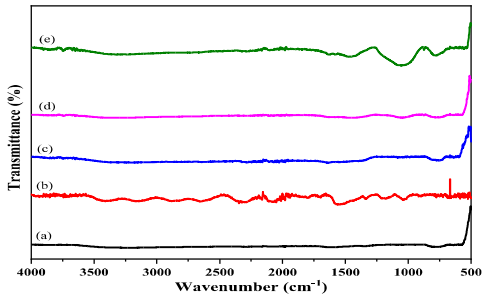

Fig. 6: FTIR spectra of TiO_2 (a), CNTs (b), TiO_2/CNTs (9:1) (c), TiO_2/CNTs (7:3) (d), TiO_2/CNTs (5:5) (e)

4 CONCLUSION

The results presented in this study showed that TiO_2/CNTs nanocomposites are reliable filler candidates for compounding hybrid nanofluids for machining processes. Characterisation results showed that the NPs are in good shape for the reinforcement base-oils from both organic and inorganic sources for the formulation of nanofluids meant for machining CFRPs. The sites created following the functionalization of CNTs (fibre) filled by TiO_2 (particles); making the formulation of nanosuspension system less challenging. The tendency of agglomeration in CNT system is significantly reduced as TiO_2 NPs occupy certain sites on the walls of CNTs and breaks the van der Walls attractions between individual CNTs. Three different nanofiller ratios were investigated under the same conditions and it was found that the stability of the nanofluids for machining application was significantly improved by the addition of fillers with TiO_2/CNTs (7:3) NCs being the most stably dispersed of the three as could be noticed with the HRSEM micrographs. The clustering simply indicates that the openings on the walls of CNTs attract TiO_2 in the suspension. Generally, however, the results from HRSEM/EDX, XRD and BET show that TiO_2/CNTs (5:5) NC offers an overriding advantage over other NCs as heat removing materials from the machining zone. The resulting nanosuspension is expected to be employed to reinforce base-oils for machining purposes.

ACKNOWLEDGEMENT

The authors thankfully acknowledge the support of the Tertiary Education Trust Fund, Nigeria, through the National Research Fund (NRF) with grant number: TETF/ES/DR&D/CE/NRF2020/SETI/113/VOL.1 for funding this research.

REFERENCES

Abubakre, O. K., Medupin, R. O., Akintunde, I. B., Tijani, J. O., Abdulkareem, A. S., Muriana, R. A., James, J. A., Ukoba, K. O., Jen, T-C., & Yoro, K. O. (2023). Journal of Science: Advanced Materials and Devices Carbon nanotube-reinforced polymer nanocomposites for sustainable biomedical applications: A review. *Journal of Science: Advanced Materials and Devices*, *8*(2), 100557. https://doi.org/10.1016/j.jsamd.2023.100557

Agrawal, S. M., & Patil, N. G. (2018). Experimental study of non-edible vegetable oil as a cutting fluid in machining of M2 Steel using MQL. *Procedia Manufacturing*, *20*, 207–212. https://doi.org/10.1016/j.promfg.2018.02.030

Bai, X.; Li, C.; Dong, L. & Yin, Q. (2019). Experimental evaluation of the lubrication performances of different nanofluids for minimum quantity lubrication (MQL) in milling Ti-6Al-4V. *International Journal of Advanced Manufacturing Technology*, 101, 2621–2632.

Brockmann, E. C., Pyykko, M., Hannula, H., Khan, K., Lamminmaki, U. & Huovinen, T. (2020). Combinatorial mutagenesis with alternative CDR-L1 and H2 loop lengths contributes to affinity maturation of antibodies, *New Biotechnology*, 60, 173-182, https://doi.org/10.1016/j.nbt.2020.09.002

D'Aloia, A. G., Di Fransesco, A. & De Santis, V. (2021). A novel computational method to identify/analyse hysteresis loops of hard magnetic materials, *Magnetochemistry*, 7(10), https://doi.org/10.3390/megnetochemistry7010010

Elgnemi, T. S. M., Jun, M. B. G., Songmene, V., & Samuel, A. M. (2021). Milling performance of CFRP composite and atomised vegetable oil as a function of fibre orientation. *Materials*, *14*(8). https://doi.org/10.3390/ma14082062

Erturk, A. T., Yarar, E., Vatansever, F., Sahin, A. E., Kilinçel, M., & Alpay, Y. O. (2021). A comparative study of mechanical and machining performance of polymer hybrid and carbon fiber epoxy composite materials. *Polymers and Polymer Composites*, *29*(9), S655–S666. https://doi.org/10.1177/09673911211020620

Gao, T. et al. (2020). Surface morphology assessment of CFRP transverse grinding using CNT nanofluid minimum quantity lubrication. J. Clean. Prod. 277, 123328. https://doi.org/10.1016/j.jclepro.2020.123328

Gao, T., Zhang, Y., Li, C., Wang, Y., An, Q., Liu, B., Said, Z., & Sharma, S. (2021). Grindability of carbon fiber reinforced polymer using CNT biological lubricant. *Scientific Reports*, *11*(1), 1–14. https://doi.org/10.1038/s41598-021-02071-y

Gopiraman, M., Selvakumaran, N., Kesavan, D., Kim, I. S., & Karvembu, R. (2012). Chemical and physical interactions of 1-benzoyl-3,3-disubstituted thiourea derivatives on mild steel surface: Corrosion inhibition in acidic media. *Industrial and Engineering Chemistry Research*, *51*(23), 7910–7922. https://doi.org/10.1021/ie300048t

Haq, M. A., Hussain, S., Ali, M. A., Farooq, M. U., Mufti, N. A., Pruncu, C. I., & Wasim, A. (2021). Evaluating the effects of nano-fluids based MQL milling of IN718 associated to sustainable productions. *Journal of Cleaner Production*, *310*(May), 127463. https://doi.org/10.1016/j.jclepro.2021.127463

Jamil MKhan, A. M. & Hegab, H. (2020). Milling of Ti–6Al–4V under hybrid Al_2O_3-MWCNT nanofluids considering energy consumption, surface quality, and tool wear: A sustainable machining, *International Journal Advanced Manufacturing Technology*, 107, 4141–4157.

Khadom, A. A., Abd, A. N., Ahmed, N. A., Kadhim, M. M., & Fadhil, A. A. (2022). Combined influence of iodide ions and Xanthium Strumarium leaves extract as eco-friendly corrosion inhibitor for low-carbon steel in hydrochloric acid. *Current Research in Green and Sustainable Chemistry*, *5*(December 2021), 100278. https://doi.org/10.1016/j.crgsc.2022.100278

Kumar, A., Sharma, A. K. & Katiyar, J. K. (2023). State-of-the-art in sustainable machining of different materials using nano minimum quality lubrication (NMQL), *Lubricants, 11, 64. https://doi.org/10.3390/lubricants11020064*

Lawal, S.A., Medupin, R. O., Yoro, K. O., Okoro, U. G., Adedipe, O., Abutu, J., Tijani, J. O., Abdulkareem, A. S., Ukoba, K., Ndaliman, M. B., Sekoai, P. T. & Jen, T-C. (2023). Nanofluids and their application in carbon fibre reinforced plastics: A review of properties, preparation and usage, *Arabian Journal of Chemistry*, 16, 104908, https://doi.org/10.1016/j.arabjc.2023.104908

Ma, C., Wen, R., Zhou, F., Zhao, H., Bao, X., Evelina, A., Long, W., Wei, Z., Ma, L., Liu, J., & Chen, S. (2022). Preparation and application of an environmentally friendly compound lubricant based biological oil for drilling fluids. *Arabian Journal of Chemistry*, *15*(3), 103610. https://doi.org/10.1016/j.arabjc.2021.103610

Medupin, R. O., Abubakre, O. K., Abdulkareem, A. S., Muriana, R. A., & Abdulrahman, A. S. (2019). Carbon Nanotube Reinforced Natural Rubber Nanocomposite for Anthropomorphic Prosthetic Foot Purpose. *Scientific Reports*, *9*(1). https://doi.org/10.1038/s41598-019-56778-0

Medupin, R. O., Abubakre, O. K., Abdulkareem, A. S., Muriana, R. A., Kariim, I., & Bada, S. O. (2017). Thermal and physico-mechanical stability of recycled high-density polyethylene reinforced with oil palm fibres. *Engineering Science and Technology, an International Journal*, *20*(6), 1623–1631. https://doi.org/10.1016/j.jestch.2017.12.005

Medupin, R. O., Abubakre, O. K., Abdulkareem, A. S., Muriana, R. A. & Lawal, S. A, (2020). Dimensional and Thermal Reliability of Multi-Walled Carbon Nanotube Filled Natural Rubber Nanocomposites, *International Journal of Engineering Research in Africa*, 51, 177-189

Mustapha, S., Ndamitso, M. M., Abdulkareem, A. S., Tijani, J. O., Shuaib, D. T., Ajala, A. O., & Mohammed, A. K. (2020). Application of TiO_2 and ZnO nanoparticles immobilized on clay in wastewater treatment: a review. *Applied Water Science*, 10(1). Springer International Publishing. https://doi.org/10.1007/s13201-019-1138-y

Ni, J., Cui, Z., Wu, C., Sun, J., & Zhou, J. (2021). Evaluation of MQL broaching AISI 1045 steel with sesame oil containing nano-particles under best concentration. *Journal of Cleaner Production*, 320(May), 128888. https://doi.org/10.1016/j.jclepro.2021.128888

Osman, K. A., Yılmaz, V., Ünver, H. Ö., ¸Seker, U. & Kılıç, S. (2020). Slot milling of titanium alloy with hexagonal boron nitride and minimum quantity lubrication and multi-objective process optimization for energy efficiency. *Journal of Cleaner Production*, 258, 120739.

Patole, P. B., Pol, G. J., Desai, A. A., & Kamble, S. B. (2021). Analysis of surface roughness and cutting force under MQL turning using nano fluids. *Materials Today: Proceedings*, *45*, 5684–5688. https://doi.org/10.1016/j.matpr.2021.02.501

Paumo, H.K., Dalhatou, S., Katata-Seru, L.M., Kamdem, B.P., Tijani, J.O., Vishwanathan, V., Kane, A., & Bahadur, I. (2021). TiO_2 assisted photocatalysts for degradation of emerging organic pollutants in water and wastewater. *Journal of Molecular Liquids*, 331, 115458. https://doi.org/10.1016/j.molliq.2021.115458

Shaban, M. M., Eid, A. M., Farag, R. K., Negm, N. A., Fadda, A. A., & Migahed, M. A. (2020). Novel trimeric cationic pyrdinium surfactants as bi-functional corrosion inhibitors and antiscalants for API 5L X70 carbon steel against oilfield formation water. *Journal of Molecular Liquids*, 305, 112817. https://doi.org/10.1016/j.molliq.2020.112817

Singh, Y., Negi, P., Yadav, A., & Tripathi, R. (2021). Euphorbia lathyris: A novel feedstock for bio based lubricant application with titanium dioxide nanoparticles as additives. *Materials Today: Proceedings*, 46, 10518–10522. https://doi.org/10.1016/j.matpr.2020.12.1237

Urmi, W. T., Shafiqah, A. S., Rahman, M. M., Kadirgama, K., & Maleque, M. A. (2021). Preparation Methods and Challenges of Hybrid Nanofluids: A Review. *Journal of Advanced Research in Fluid Mechanics and Thermal Sciences*, 78(2), 56–66. https://doi.org/10.37934/ARFMTS.78.2.5666

Usha, M., & Srinivasa Rao, G. (2019). Optimisation of Parameters in Turning Using Herbal Based Nano Cutting Fluid with MQL. *Materials Today: Proceedings*, *22*, 1535–1544. https://doi.org/10.1016/j.matpr.2020.02.115

Venkatesan, K., Devendiran, S., Sachin, D., & Swaraj, J. (2020). Investigation of machinability characteristics and comparative analysis under different machining conditions for sustainable manufacturing. *Measurement: Journal of the International Measurement Confederation*, 154, 107425. https://doi.org/10.1016/j.measurement.2019.107425

Wang, J. J., Zhang, J. F., Feng, P. F. & Guo, P. (2018). Damage formation and suppression in rotary ultrasonic machining of hard and brittle materials: A critical review. *Ceramic International,* 44(2), 1227–1239. https://doi.org/10.1016/j.ceramint.2017.10.050

Zhang, M.J. et al. (2017). Analysis of flow field in cutting zone for spiral orderly distributed fibre tool. *International Journal of Advanced Manufacturing Technology*, 92(9–12), 4345–4354. https://doi.org/10.1007/s00170-017-0471-2

Zheng, H., Zhang, W., Li, B., Zhu, J., Wang, C., Song, G., Wu, G., Yang, X., Huang, Y., & Ma, L. (2022). Recent advances of interphases in carbon fiber-reinforced polymer composites: A review. *Composites Part B: Engineering*, 233, https://doi.org/10.1016/j.compositesb.2022.109639